Available online at www.sciencedirect.com
SCIENCE DIRECT®
Journal of Inorganic Biochemistry 98 (2004) 733–745
Journal of Inorganic Biochemistry
www.elsevier.com/locate/jinorgbio

Light-induced multistep oxidation of dinuclear manganese complexes for artificial photosynthesis

Ping Huang [a], Joakim Högblom [a], Magnus F. Anderlund [b], Licheng Sun [b,*], Ann Magnuson [a], Stenbjörn Styring [a,*]

[a] *Department of Biochemistry, Center for Chemistry and Chemical Engineering, Lund University, P.O. Box 124, Lund S-22100, Sweden*
[b] *Department of Organic Chemistry, Arrhenius Laboratories, Stockholm University, Stockholm S-10691, Sweden*

Received 22 September 2003; received in revised form 10 December 2003; accepted 11 December 2003

Abstract

Two dinuclear manganese complexes, $[Mn_2BPMP(\mu\text{-}OAc)_2]\cdot ClO_4$ (**1**, where BPMP is the anion of 2,6-bis{[*N*,*N*-di(2-pyridinemethyl)amino]methyl}-4-methylphenol) and $[Mn_2L(\mu\text{-}OAc)_2]\cdot ClO_4$ (**2**, where L is the trianion of 2,6-bis{[*N*-(2-hydroxy-3,5-di-*tert*-butylbenzyl)-*N*-(2-pyridinemethyl)amino]methyl}-4-methylphenol), undergo several oxidations by laser flash photolysis, using ruthenium^{II}-*tris*-bipyridine (tris(2,2-bipyridyl)dichloro-ruthenium(II) hexahydrate) as photo-sensitizer and *penta*-amminechlorocobalt(III) chloride as external electron acceptor. In both complexes stepwise electron transfer was observed. In **1**, four Mn-valence states from the initial $Mn_2^{II,II}$ to the $Mn_2^{III,IV}$ state are available. In **2**, three oxidation steps are possible from the initial $Mn_2^{III,III}$state. The last step is accomplished in the $Mn_2^{IV,IV}$ state, which results in a phenolate radical.

For the first time we provide firm spectral evidence for formation of the first intermediate state, $Mn_2^{II,III}$, in **1** during the stepwise light-induced oxidation. Observation of $Mn_2^{II,III}$ is dependent on conditions that sustain the μ-acetato bridges in the complex, i.e., by forming $Mn_2^{II,III}$ in dry acetonitrile, or by addition of high concentrations of acetate in aqueous solutions. We maintain that the presence of water is necessary for the transition to higher oxidation states, e.g., $Mn_2^{III,III}$ and $Mn_2^{III,IV}$ in **1**, due to a bridging ligand exchange reaction which takes place in the $Mn_2^{II,III}$ state in water solution. Water is also found to be necessary for reaching the $Mn_2^{IV,IV}$ state in **2**, which explains why this state was not reached by electrolysis in our earlier work (Eur. J. Inorg. Chem (2002) 2965).

In **2**, the extra coordinating oxygen atoms facilitate the stabilization of higher Mn valence states than in **1**, resulting in formation of a stable $Mn_2^{IV,IV}$ without disintegration of **2**. In addition, further oxidation of **2**, led to the formation of a phenolate radical ($g = 2.0046$) due to ligand oxidation. Its spectral width (8 mT) and very fast relaxation at 15 K indicates that this radical is magnetically coupled to the $Mn_2^{IV,IV}$ center.

Keywords: Manganese; Photosynthesis; Ruthenium; Electron paramagnetic resonance

1. Introduction

Solar energy is an attractive energy source and great progress has been made in converting solar energy to electricity or heat. Our work aims at utilizing solar energy for direct fuel production, and we therefore aim to design a molecular system for artificial photosynthesis [1].

Photosynthesis is the most important energy converting process in the biosphere, where sunlight is captured and stored in energy rich compounds such as carbohydrates. In oxygenic photosynthesis in cyanobacteria, algae and higher plants, Photosystem II (PSII) utilizes sunlight as driving force to extract electrons from water, which is oxidized to molecular oxygen, thereby providing electrons for the reduction of carbon dioxide. Water is, thereby, an inexhaustible electron source for the biosphere, and water oxidation in PSII is a key process in nature.

PSII is a large membrane bound protein complex with close to 30 protein subunits [2]. When the primary

* Corresponding authors. Tel.: +4646-222-0108; fax: +4646-222-4534 (Stenbjörn Styring); fax: +46-8-15-4908 (Licheng Sun).
E-mail addresses: licheng.sun@organ.su.se (L. Sun), stenbjorn.styring@biokem.lu.se (S. Styring).

0162-0134/$ - see front matter © 2003 Elsevier Inc. All rights reserved.
doi:10.1016/j.jinorgbio.2003.12.009

donor chlorophylls P_{680} in the core of PSII absorb a photon, the excited P_{680}* rapidly ejects an electron to a series of protein-bound electron acceptors. The formed P^{+}_{680} has a strongly oxidizing redox potential of ca. +1.2 V vs. NHE [3–6], and takes an electron back from the components of the water oxidizing complex (WOC) and ultimately from water. The WOC consists of a tetranuclear manganese (Mn_4) complex working in conjunction with a redox active tyrosine residue (Tyr_Z), identified as Tyr161 on the D1 protein of PSII [4,5,7,8]. The Mn_4-complex acts as a charge storing device and cycles through a series of oxidation states, S_0–S_4, with S_0 being the most reduced state [4,9–12]. For each electron ejected from P_{680}*, the WOC is oxidized one step until four electrons have been extracted. Then, two water molecules are oxidized into molecular oxygen and the Mn_4-cluster returns to S_0.

The exact molecular details of both the structure and the catalytic mechanism of the manganese complex in PSII are still unknown. It is well established, however, that several or all of the S-states transitions involve oxidation of manganese [9,10,13]. There are strong indications that water molecules bind terminally to one of the Mn-ions prior to oxidation [11,14,15]. In addition, the Mn_4-complex seems to undergo structural changes upon the transition between the S_2 and S_3 states [9,10]. Such structural changes may be necessary for the incorporation of water molecules, or involve rearrangements of bridging or terminal ligands in order to accommodate the increased charge being stored in the S-states. The involvement of μ-oxo bridges between the Mn-ions is supported by EXAFS, but it is also highly likely that carboxylic groups from bicarbonate or amino acid side chains are bridging the Mn-ions in the WOC [7,9,10,16].

We aim at mimicking the essential structural and functional parts of the Mn_4–Tyr ensemble to develop artificial photosynthesis. We, and others [1,17–20], have synthesized multinuclear ruthenium–manganese model complexes as functional mimics of the WOC. In our systems we use ruthenium^{II}-*tris*-bipyridine ($Ru^{II}(bpy)_3$) complexes as photo-sensitizer (to mimic the function of P_{680}) coupled to redox active Mn-moieties that are intended to mimic the Mn_4-complex in PSII. We recently demonstrated that a dinuclear Mn complex, **1** (Scheme 1), [1] either free or covalently linked to a $Ru^{II}(bpy)_3$ complex, could be oxidized several steps from $Mn_2^{II,II}$ to $Mn_2^{III,IV}$ via light-induced electron transfer to a Ru-center that was photo-oxidized in the presence of an electron acceptor [20,21]. The complete reaction could only take place in the presence of water and our hypothesis was that an exchange of the bridging ligands

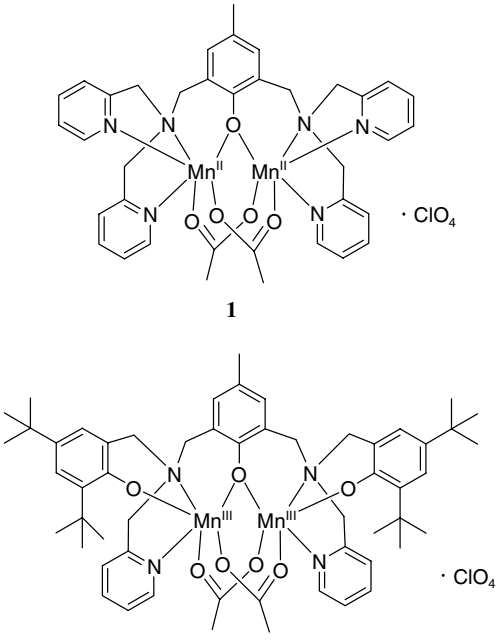

Scheme 1.

takes place prior to formation of the higher oxidation states, likewise to what has been observed in similar systems [22]. We thus demonstrated that it is possible to mimic the electron transfer reactions in PSII.

In **1**, the manganese dimer is coordinated to bpmp, which has a well-known ligand sphere [23–25]. The two manganese ions in **1** are bridged via a phenoxyl group and two terminal acetate molecules. Interestingly, water is required for obtaining the $Mn_2^{III,IV}$ state. From EPR and electrochemistry, and lately also from EXAFS investigations, we have concluded that water induces a change in the bridging mode between the Mn-ions, which is necessary for efficient formation of the $Mn_2^{III,IV}$ state ([21]; A. Magnuson, H. Dau et al., in preparation). The change in bridging mode includes a loss of one or both acetate ligands, and the formation of one or two new μ-oxo bridges. We did not observe any formation of higher oxidation states than $Mn_2^{III,IV}$.

In an attempt to increase the similarity between our synthetic systems and the Mn_4-complex in PSII, we constructed a novel dinuclear Mn_2-complex **2**, similar to **1**, but with a ligand set where two of the pyridine groups in **1** had been exchanged for phenol groups (Scheme 1) [26]. With its phenolate ligands and higher O/N ratio, the electron donating properties of the ligand sphere increases, and it can be expected that higher oxidation states will be more stabilized in **2** compared to **1**. Electrochemical measurements of **2** showed that it is possible to accommodate up to five separate oxidation states in this complex. In contrast to **1**, the $Mn_2^{III,IV}$ state can be reached in **2**, also in the absence of water [26].

[1] The notation **1** and **2** for the structure of the dinuclear manganese complexes are used for all oxidation states, even if the terminal di-μ-acetato bridges are exchanged in the higher oxidation states (see text).

The unique property of PSII, which enables it to oxidize water, is its capacity to generate and store four oxidizing equivalents before oxidizing two water molecules and releasing molecular oxygen. Therefore, to create a truly bio-mimetic system for artificial photosynthesis and water-oxidation, the donor system (i.e., the manganese complex) must be able to deliver four electrons to the photo-sensitizer.

In the present study, we have made further investigations of the chemical properties of the two Mn_2-complexes **1** and **2** (Scheme 1). We examine all the intermediates observed during photo-induced oxidation of both **1** and **2** in the presence of $Ru^{II}(bpy)_3$ as photo-sensitizer and an electron acceptor. We show the EPR spectra of the EPR observable intermediates and we are now able to present a better resolution of the intermediate steps in the stepwise photo-induced oxidation of **1**. Thereby, we reinforce the ligand exchange mechanism, which we propose is necessary for reaching higher oxidation states in **1**. We also demonstrate that oxidation of **2**, induced by a photo-sensitizer, allows the generation of higher oxidation states in **2** than in **1**, supporting the idea that the phenolates in **2**, providing a higher O/N ratio, stabilizes higher oxidation states. In addition, a neutral phenol radical is formed in **2**, which offers interesting analogies to the WOC in PSII.

2. Experimental

2.1. Chemicals and synthesis

Penta-amminechlorocobalt(III)chloride, Co^{III}, was purchased from Aldrich. $Ru^{II}(bpy)_3$ was purchased from Aldrich (tris(2,2′-bipyridyl)dichloro-ruthenium(II) hexahydrate), or prepared according to Sullivan and Meyer [27]. Complex **1** in the $Mn_2^{II,II}$ and $Mn_2^{II,III}$ states was synthesized according to Diril et al. [23] and modified as by Sun et al. [20], and **2** was prepared as described in [26]. 4-Nitrobenzyl bromide (4-NBB) (99%) was purchased from Acros. $Mn_2^{III,IV}(bpy)_4O_2$ was synthesized as in [28].

2.2. EPR spectroscopy

X-band EPR measurements were performed on a Bruker E580 ELEXSYS spectrometer equipped with a rectangular dual mode resonator and an Oxford Instruments ESR 900 flow cryostat. EPR spectra were analysed using the XEPR software package. Laser flashes at 5 Hz and 532 nm (6 ns pulse width, ~250 mJ/flash) were given at room temperature from a frequency doubled Spectra Physics DCR 3G Nd:YAG laser. The incident laser light was adjusted with lenses to cover the entire EPR sample volume.

For the EPR studies, **1** and $Ru^{II}(bpy)_3$ were dissolved in acetonitrile. A saturated Co^{III}-solution in buffered water (200 mM sodium acetate buffer, pH 4.6) was obtained as described in [21]. The stock solution of **1** and $Ru^{II}(bpy)_3$ in acetonitrile was mixed with the Co^{III} solution to final concentrations of 1.8, 2.4 and 18 mM, respectively. After mixing, the sample contained 10% (v/v) acetonitrile. The solution was transferred to EPR tubes and the samples were immediately frozen in an ethanol/dry ice bath ($T = 198$ K), and then transferred to 77 K for storage before EPR examination. All solvents and solutions were purged with argon before use and kept deoxygenated throughout the experiments. The EPR samples were prepared under dim red light to avoid unwanted photo-reactions and care was taken to minimize the interval between mixing and freezing of the samples (mix-freeze time <1 min).

In the photochemical experiments, saturating laser flashes (5 Hz repetition rate) were applied to the pre-thawed EPR samples at room temperature. After the designated number of flashes, the sample was frozen in an ethanol/dry ice bath within 2 s and then quickly transferred to liquid N_2 until further use. X-band EPR spectra were recorded before and after flash illumination of the EPR samples.

Photochemical studies of **2** were carried out in essentially the same way. Complex **2** dissolved in acetonitrile was mixed with $Ru^{II}(bpy)_3$ and saturated Co^{III} in water solution to final concentrations of 1, 4 and 8 mM, respectively. After mixing, the sample contained 50% (v/v) acetonitrile. Further handling of the samples was done as described for **1**. The stability of **2** in water was tested by storing **2** (at 1 mM concentration) in mixtures of acetonitrile and water for 30 s at room-temperature before freezing and recording of EPR spectra.

The $Mn_2^{II,II}$ component of **1** was quantified in the EPR spectra from comparison with a reference $Mn_2^{II,II}$ spectrum from a known concentration of **1** in acetonitrile. Specifically, the peak height at 261 mT ($g \sim 2.6$) (compare Fig. 1(a)), characteristic for $Mn_2^{II,II}$ was used for the quantification. The $Mn_2^{II,III}$ component, of **1** in the photo-chemically treated samples was quantified from comparison with the EPR spectrum of **1** synthetically prepared in the $Mn_2^{II,III}$ state (1 mM) in neat acetonitrile. The peak height of a series of hyperfine lines in the 380–460 mT region, that clearly originate from $Mn_2^{II,III}$ bpmp (see text), were used for the quantification.

To quantify the $Mn_2^{III,IV}$ component of **1** and **2**, that have not been synthesized in this oxidation state, we used $Mn_2^{III,IV}(bpy)_4O_2$ as reference complex [28]. The concentration of $Mn_2^{III,IV}(bpy)_4O_2$ in acetonitrile was determined by UV–Vis spectrophotometry, using the extinction coefficient $\varepsilon = 900\ M^{-1}\,cm^{-1}$ at $\lambda = 687$ nm [28]. The EPR signal intensity from this standard sample (recorded at the appropriate microwave power and

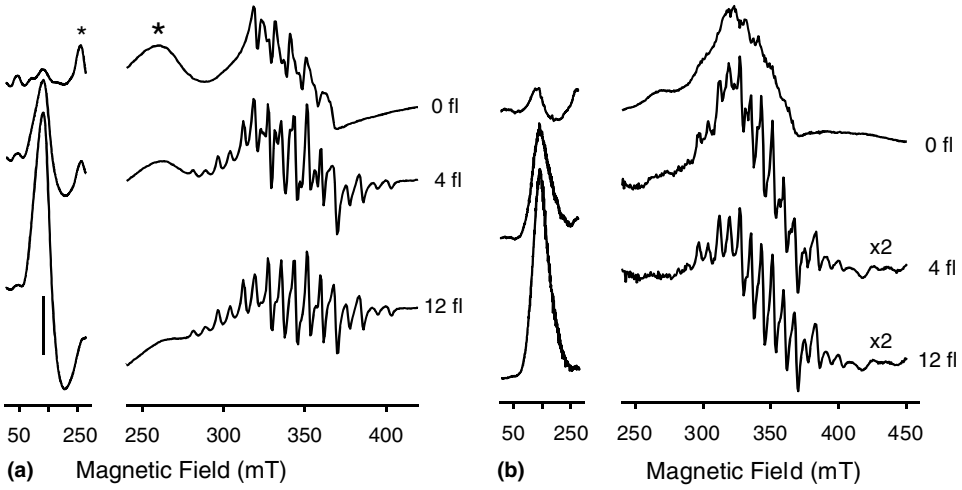

Fig. 1. EPR spectra, which demonstrate the formation and decay of intermediate redox states during photo-induced oxidation of **1** by $Ru^{II}(bpy)_3$ in the presence of Co^{III} as electron acceptor in 10% (v/v) acetonitrile in acetate buffer. (a) Spectra recorded at 12 K, 12 mW microwave power to enhance the EPR signal from the $Mn_2^{II,II}$ and $Mn_2^{III,IV}$ states. (b) Spectra recorded at 4 K, 159 mW microwave power to enhance the EPR signal from $Mn_2^{II,III}$. The lower spectra (4 and 12 fl spectra) are multiplied by a factor of 2 to better visualize the spectral features in the $Mn_2^{II,III}$ spectra. In both (a) and (b), compressed spectra in the range 0–300 mT are shown on the left and expanded spectra that resolve the EPR spectra from the Mn-dimer in the 240–420 mT range are shown on the right. The spectra in each panel were recorded in the same samples which had been exposed to 0, 4 and 12 laser flashes. The asterisk at 261 mT in (a) shows the position of the peak from the $Mn_2^{II,II}$ spectrum that was used to estimate the concentration of this component. The bar indicates the peak position at 132 mT of the Co^{II} signal formed by photo-induced reduction of Co^{III}. EPR settings: Frequency, 9.62 GHz; modulation frequency, 100 kHz; modulation amplitude, 1 mT.

temperature to allow direct comparison) was then compared to the signal intensities in selected EPR spectra from **1** or **2** where the $Mn_2^{III,IV}$ signal dominates. This occurred in the case of **1**, in the spectrum of a sample that had been exposed to 12 flashes, when the spectrum was recorded at 12 K (see Fig. 1(a), 12 fl). In the case of **2** this occurred after 150 flashes (Fig. 5(a), 150 fl). In those samples, the concentration of $Mn_2^{III,IV}$ was determined by comparison with the reference compound. In other samples, where the spectra represented a mixture of several valence states, the concentration of $Mn_2^{III,IV}$ was determined from the amplitudes of selected, easily identifiable hyperfine lines (see text). It should be pointed out that the use of a different compound than **1** or **2** as reference compound can give rise to errors due to different chemical and spectroscopic properties of the compounds. However, any error introduced should be small and is systematic for a given compound. Thus, the trends for induction and decay of $Mn_2^{III,IV}$ in the flash series (see below) will be correct and this is very important for the mechanistic considerations in the paper.

3. Results

3.1. Stepwise photo-oxidation of *1* in the presence of water

It was demonstrated previously [21] that photo-oxidation of $Ru^{II}(bpy)_3$ to $Ru^{III}(bpy)_3$ resulted in subsequent oxidation of **1** from the initial $Mn_2^{II,II}$ to the $Mn_2^{III,IV}$ valence state in a stepwise fashion. The general formulas for the photo-induced reactions are described in reactions (1) and (2), where the step from Mn_2^{RED} to Mn_2^{OX} represents oxidation of the Mn dimer one step

$$Ru^{II}(bpy)_3 + Co^{III} \xrightarrow{h\nu} Ru^{III}(bpy)_3 + Co^{II} \quad (1)$$

$$Ru^{III}(bpy)_3 + Mn_2^{RED} \rightarrow Ru^{II}(bpy)_3 + Mn_2^{OX} \quad (2)$$

In our previous study we were unable to detect the EPR spectrum from $Mn_2^{II,III}$ as a firm evidence that $Mn_2^{II,III}$ is an intermediate state via which **1** undergoes stepwise photo-induced oxidation from $Mn_2^{II,II}$ to $Mn_2^{III,IV}$. It also seemed that $Mn_2^{III,IV}$ was the highest valence state that could be reached. In the present work, our aim was to follow the light-induced formation and decay of intermediates during oxidation of **1** and to investigate if the $Mn_2^{III,IV}$ state could be further oxidized. To manage this, all EPR spectra from all samples were recorded under a set of recording conditions that each highlights one or the other of the oxidation states. This is necessary since many of the resulting EPR spectra contain several EPR active species, which complicate the quantitative analysis of each individual component. In addition, the experiments were performed in acetate buffer to modify ligand exchange equilibria, thereby creating a situation where intermediates possibly would be easier to detect.

Fig. 1 shows a selection of our data, where all spectra in panel (a) were recorded at 12 K and intermediate microwave power (12 mW), which allows quantification of the $Mn_2^{II,II}$ and $Mn_2^{III,IV}$ states. Fig. 1(b) shows spectra

from the very same samples but recorded at 4 K and high microwave power (159 mW), which allows quantification of the $Mn_2^{II,III}$ state. In the dark, the EPR spectrum of **1** (1.8 mM) recorded at 12 K was typical for dimeric $Mn_2^{II,II}$ which has wide spectral features up to 700 mT (Fig. 1(a), 0 fl) [29,30]. The amplitude of the peak at 261 mT ($g \sim 2.6$), marked with an asterisk, was chosen to monitor the change of $Mn_2^{II,II}$ when the dark sample was exposed to flashes. This $Mn_2^{II,II}$ spectrum was superimposed on a 6-line signal in the $g \sim 2$ regions that arises from a small fraction of monomeric Mn^{II} (ca. 5%, ~0.1 mM; similar to what has been observed earlier [21]). The spectral features at 12 K of **1** in the $Mn_2^{II,II}$ state arise from transitions of spin triplets and quintets due to weak anti-ferromagnetic exchange interactions between the two Mn^{II} ions [29,30]. These transitions vanish at very low temperature at which the EPR inactive $S = 0$ ground state is mostly populated. Indeed, the EPR spectrum of the dark sample recorded at 4 K is dominated by a broad 6-line signal that stems from the small contamination of Mn^{II} (Fig. 1(b), 0 fl). The $Mn_2^{II,II}$ signal is seen as a weak shoulder at the left side of the strong 6-line signal.

Following excitation by a laser flash, the excited $Ru^{II}(bpy)_3$ transfers one electron to Co^{III}. The formed $Ru^{III}(bpy)_3$ then retrieves one electron from the Mn moiety of **1** [reactions (1) and (2)]. The electron transfer to Co^{III} can be monitored by the formation of Co^{II}, which has an EPR signal at $g \sim 5.2$ (Fig. 1(a), peak marked with a bar at 132 mT). The Co^{II} signal increases when a sequence of laser flashes is applied and is present in all EPR spectra of the flashed samples.

The oxidation of **1** leads to a decrease of the initial $Mn_2^{II,II}$ oxidation state with the simultaneous formation of higher oxidation states. The selected spectra shown in Fig. 1(a) and (b) were recorded after 4 and 12 flashes were applied, respectively, and show how the Mn_2-derived EPR signals come and go. The data from the spectra in Fig. 1 and from the same samples exposed to a varied number of flashes are compiled in Fig. 2 that shows the quantitative analysis of the Mn-valence state composition during the entire flash series. After 2 flashes, ~40% of the $Mn_2^{II,II}$ signal had disappeared (Fig. 2). After 2 more flashes, another 14% of $Mn_2^{II,II}$ disappeared (Fig. 1(a), 4 fl). The $Mn_2^{II,II}$ signal decreased further with the applied flashes and nearly disappeared after the sample had been exposed to 12 flashes (Fig. 1(a), 12 fl; 17% remaining, Fig. 2). After 4 flashes (Fig. 1(a)), a 16-line signal centered at $g \sim 2$ appeared. It was clearly visible, though it overlapped with the remaining part of $Mn_2^{II,II}$ (~38%). The multiline signal was about 122 mT wide with 16 well-resolved lines separated by about 7.5 mT. These features are best viewed in the bottom spectrum in Fig. 1(a), where the sample had been exposed to 12 flashes and the maximal signal amplitude was detected. These spectral characteristics are

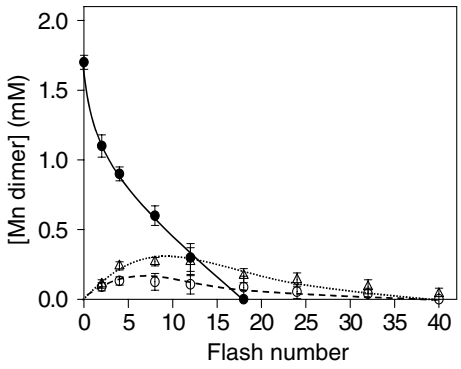

Fig. 2. Flash number dependent decrease of $Mn_2^{II,II}$ (–●–) and formation of $Mn_2^{II,III}$ (–○–) and $Mn_2^{III,IV}$ (–△–) in an experiment, where **1** was exposed to a series of laser flashes in presence of $Ru_2^{II}(bpy)_3$ and Co^{III}. The experimental conditions were as in Fig. 1. The concentration of each Mn valence state was determined from EPR spectra similar to those in Fig. 1, which were compared to EPR spectra from samples with known concentration (see Section 2).

typical for $Mn_2^{III,IV}$ [31–33] and can thus be safely assigned to **1** in the $Mn_2^{III,IV}$ valence state being formed as a result of photo-oxidation. The maximal amount of $Mn_2^{III,IV}$ was ~0.3 mM after 12 flashes. In essence, this light-induced formation of $Mn_2^{III,IV}$ from $Mn_2^{II,II}$ is similar to that in our previous study [21]. The same holds for the disappearance of the 6-line signal from Mn^{II} that was essentially gone after ca. 10 flashes.

Fig. 1(b) shows the same samples measured at 4 K. At this temperature the EPR spectrum of the sample that had been exposed to 2 flashes (not shown) showed spectral features different from the 16-hyperfine lines of $Mn_2^{III,IV}$. The new signal increased after 2 more flashes, and the EPR spectrum of the 4-flash sample is shown in Fig. 1(b), middle spectrum. This spectrum shows new hyperfine lines centered at $g \sim 2$. The hyperfine line pattern in the region 380–460 mT is quite clean from overlapping signals and allows us to assign this signal to the $Mn_2^{II,III}$ oxidation state of **1** (see below). The spectrum is not as well resolved in the lower (<300 mT) field region. Despite the complication of the spectral analysis, the clearly resolved hyperfine pattern in the region between 380–460 mT (Fig. 1(b), middle and bottom) allows identification of the species giving rise to the spectrum as **1** in the $Mn_2^{II,III}$ state. This is shown in Fig. 3, where the spectrum from **1**, chemically prepared as $Mn_2^{II,III}$ (Fig. 3, spectrum b), is shown together with parts of the 4-flash spectrum from Fig. 1(b) (Fig. 3, spectrum a). The easily recognized large hyperfine lines from $Mn_2^{II,III}$ are clearly the same as those found in the 4-flash spectrum (rasterized lines are identical). These lines are "clean" enough to allow determination of the concentration of the $Mn_2^{II,III}$ present in the spectra from the flash series. The remaining part of the spectrum is a mix of several species (Mn^{II}, $Mn_2^{II,III}$ and $Mn_2^{III,IV}$) and any analysis of the $Mn_2^{II,III}$ fraction is difficult.

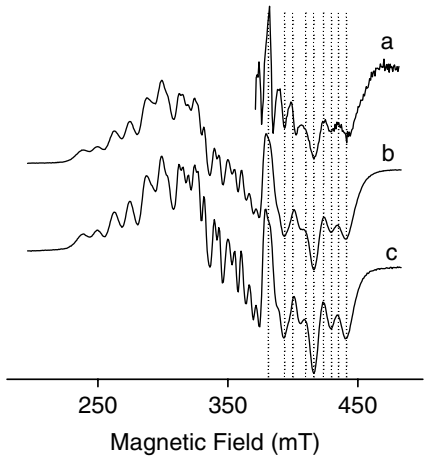

Fig. 3. EPR spectra of $Mn_2^{II,III}$ obtained under various conditions. Spectrum a is the same as in Fig. 1(b), 4 fl, but for clarity only lines between 380 and 460 mT are shown to allow comparison with resolved spectra of $Mn_2^{II,III}$ in (b) and (c). Spectrum b was recorded in a sample with Mn_2(bpmp) synthetically prepared in the $Mn_2^{II,III}$ state. Spectrum c was recorded after giving 50 flashes to a sample of **1** in neat acetonitrile in the presence of $Ru^{II}(bpy)_3$ and 4-NBB. The raster indicates the hyperfine lines from $Mn_2^{II,III}$, which allow identification and quantification of $Mn_2^{II,III}$ in mixed spectra with contributions from Mn^{II} and $Mn_2^{III,IV}$.

From comparison of the various EPR signals with control samples of **1** in the different oxidation states, we have determined the flash dependent evolution of the $Mn_2^{II,II}$ into the $Mn_2^{II,III}$ state and subsequently the formation and disappearance of the $Mn_2^{III,IV}$ state. The results are compiled in Fig. 2. The efficiency for oxidation of $Mn_2^{II,II}$ was high after each flash. After 2 flashes ca. 40% of $Mn_2^{II,II}$ was oxidized, and after 10–12 flashes ca. 80% of $Mn_2^{II,II}$ had been oxidized. After 4 flashes the maximum concentration of $Mn_2^{II,III}$, ~0.15 mM, was found in the sample. The signal from the $Mn_2^{II,III}$ then decreased and became undetectable after 32 flashes.

The product from oxidation of the $Mn_2^{II,III}$ is very likely the $Mn_2^{III,III}$ state. Unfortunately, when **1** is in the $Mn_2^{III,III}$ valence state it has no detectable EPR signal, neither in parallel mode nor perpendicular mode EPR. Consequently, it cannot be followed directly. In contrast, it is easy to follow and quantify the next oxidation state, $Mn_2^{III,IV}$, by the appearance of the large EPR signal (see, for example, Fig. 1(a), 12-flash spectrum). The $Mn_2^{III,IV}$ state was slowly built up and was maximal after 12–15 flashes (Fig. 2). After 12 flashes, it amounted to 0.32 mM, while the $Mn_2^{II,III}$ state was 0.1 mM and $Mn_2^{II,II}$ was 0.34 mM. Thus, almost 60% of the initially available **1** (1.7 mM) was present in an EPR invisible form. It is most likely that the $Mn_2^{III,III}$ state is the dominating form in the sample that had been exposed to 12 flashes.

When more light was applied, the situation again changed in the sample and **1** was oxidized even further. All distinguishable EPR signals from $Mn_2^{II,II}$ and $Mn_2^{II,III}$ had disappeared after 32 flashes. The signal from $Mn_2^{III,IV}$ also decreased and after ca. 40 flashes this signal was below the detection limit. The light dependent disappearance of the $Mn_2^{III,IV}$ was not accompanied by the formation of any new EPR signals from manganese. However, it was associated with formation of a dark precipitate from, what was probably, MnO_2. The formation of the precipitate increased with the number of applied flashes, when the $Mn_2^{III,IV}$ signal had started to decline. After 12 flashes however, the sample was still clear and contained no observable MnO_2. Therefore, MnO_2 is not formed from the $Mn_2^{III,IV}$ valence state. Instead it was formed from an oxidation product of $Mn_2^{III,IV}$, most probably an unstable $Mn_2^{IV,IV}$ dimer. After 30–40 flashes, the precipitation was substantial and clearly visible.

3.2. Photo-oxidation of *1* in acetonitrile

In our previous studies [21] we have used Co^{III} as electron acceptor. Since the reduction of Co^{III} to Co^{II} is irreversible in our chosen acceptor, the use of Co^{III} prevents recombination, allowing observation of oxidized Mn-states despite the low time resolution in the freeze quench experiments. However, Co^{III} has to be dissolved in water and we have been restricted to work in solutions containing water. We have, therefore, also tried 4-nitrobenzyl bromide (4-NBB), which is soluble in acetonitrile, as an electron acceptor. In our experiment we followed the photo-oxidation of **1** in the presence of 4-NBB and $Ru^{II}(bpy)_3$ (1.30 and 5 mM, respectively, in acetonitrile). In the dark, the typical EPR spectrum from $Mn_2^{II,II}$ in acetonitrile spectrum was found (not shown, but see Fig. 3 in [21]). The oxidation of **1** to $Mn_2^{II,III}$ with the laser flashes was clearly observed. After 50 flashes, we obtained a maximal signal intensity of the $Mn_2^{II,III}$ EPR spectrum, that amounted to 1 mM of $Mn_2^{II,III}$ (Fig. 3(c)). This spectrum is virtually identical to the spectrum recorded for **1** in the chemically prepared $Mn_2^{II,III}$ state (Fig. 3(b); see also [23]). The signal intensity decreased with further flashes without any new signal appearing. No $Mn_2^{III,IV}$ multiline signal could be detected (not shown). After 200 flashes there was still a substantial $Mn_2^{II,III}$ signal remaining in the spectrum, but the complex seemed to become partially destroyed as indicated by the formation of a 6-line EPR signal from Mn^{II} (not shown). We conclude that **1** can be partially oxidized to $Mn_2^{III,III}$ but not to $Mn_2^{III,IV}$ in neat acetonitrile.

3.3. Stability of *2*

The initial oxidation state of **2** is $Mn_2^{III,III}$ which is EPR silent [26]. However, in the presence of water a

6-line EPR signal from Mn^{II} appears, similar to what was earlier observed in **1** ([21], Fig. 1). It seems that water causes destruction of **2** to some extent. However, water is important for our study since we were interested in the role of the water in the photo-induced oxidation of our complexes. Besides, it is necessary to involve sufficient electron acceptor as Co^{III}, which is soluble in water but insoluble in acetonitrile, to achieve efficient electron transfer. Thus, in order to perform the experiment there is an optimal balance between the water content and stability of **2**. We, therefore, monitored the appearance of Mn^{II} versus the water content in order to find optimal conditions for photo-induced oxidation of **2** (Fig. 4). The release of Mn^{II}, during 30 s incubation was negligible ($\sim$0.02 mM) when the water content was <20% (v/v). However, this limits the concentration of Co^{III} to merely $\sim$3 mM which would not be enough to achieve efficient electron transfer. We found that 50% water in acetonitrile is a useful balance point for these photolysis experiments, where the appearance of Mn^{II} is at $\sim$0.2 mM (20% of **2**) indicating a destruction of **2** to a reasonable level. Fifty percent water also permits the use of $\sim$8 mM Co^{III} that is high enough to achieve efficient photo-induced redox reactions. It should also be emphasized, that the appearance of Mn^{II} was maximal after less than 30 s incubation at room temperature. Further incubation up to ca. 5 min, which is similar to the incubation times involved in the flash series experiments did not result in any significant increase of the Mn^{II} signal.

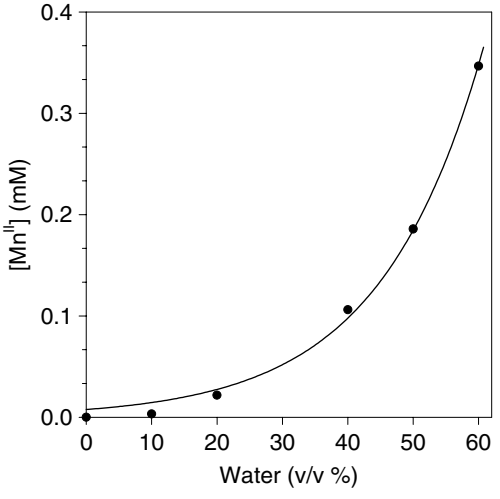

Fig. 4. Stability of **4** in water containing acetonitrile. When **2** is dissolved in water this results in appearance of Mn^{II} as revealed by an increased 6-line EPR signal. The initial concentration of **2** was 1 mM.

3.4. Photo-induced oxidation of 2

Photo-induced oxidation of **2** was carried out in essentially the same way as described for **1**. The initial state of **2**, $Mn_2^{III,III}$, is EPR silent. However, one step photo-oxidation of **2** resulted in the $Mn_2^{III,IV}$ state, which allowed us to follow the reaction course.

Fig. 5(a) shows selected spectra recorded after different number of flashes applied to a sample containing **2**, in the presence of $Ru^{II}(bpy)_3$ and Co^{III} (1, 4 and 8 mM, respectively). The more detailed analysis on the photo-oxidation course of **2** is shown in Fig. 5(b), where the $Mn_2^{III,IV}$ concentration is plotted as a function of the number of applied flashes. The top spectrum in Fig. 5(a) was recorded before the sample was exposed to laser flashes. This spectrum shows a broad Mn^{II} 6-line EPR spectrum, which represents $\sim$0.2 mM Mn^{II} (see above). When this sample was exposed to laser flashes, this resulted in the appearance and subsequent decrease of the $Mn_2^{III,IV}$ state. This is demonstrated by the EPR spectra recorded after 50, 150 and 350 flashes (Fig. 5(a)). After 50 flashes (Fig. 5(a), spectrum 50 fl), a new multiline signal appears. After 150 flashes this signal reached its maximal intensity (spectrum 150 fl in Fig. 5(a)). The signal is centered at $g \sim 2$, has a spectral width $\sim$106 mT and consists of 23 lines separated by $\sim$12 mT in both wings of the spectrum and 9 mT in the center part of the spectrum. We assign our signal to the $Mn_2^{III,IV}$ state of **2**.

We point out that also in **2**, the signal from Mn^{II} disappeared after ca. 10 flashes. At present we cannot ascertain whether the EPR observable mono-meric Mn^{II} still remains in the organic ligand or if it is free in the solution. The situation is also likely to be different in **1** and **2**. However, the efficient oxidation of Mn^{II} (the signal disappears after a few flashes) suggests that a fraction remains in the ligand.

A more detailed analysis of how the $Mn_2^{III,IV}$ concentration varied with the flash series is shown in Fig. 5(b). The first 25 flashes resulted in formation of 0.06 mM of $Mn_2^{III,IV}$. After 50 flashes, 0.09 mM $Mn_2^{III,IV}$was formed. This corresponds to 10% of the available **2**. Hundred more flashes were needed to reach the maximum yield 0.16 mM of $Mn_2^{III,IV}$. Further flashes led to decrease of this $Mn_2^{III,IV}$ signal. After 350 flashes (Fig. 5(a)), the amount of $Mn_2^{III,IV}$ had dropped to ca. 0.06 mM and it decreased even further with continued flashing (Fig. 5(b)). In the spectrum recorded after 350 flashes, we could not observe any indication of degradation of the Mn_2-dimer nor any precipitation of MnO_2 in the sample. It is also important to note that we did not observe any new spectral features after 350 flashes, which implies that the $Mn_2^{III,IV}$ state had been converted to an EPR silent valence state.

It is interesting to speculate about the nature of this "EPR silent" state. Assuming that this second oxidation of **2**, dominating in the sample provided with 350

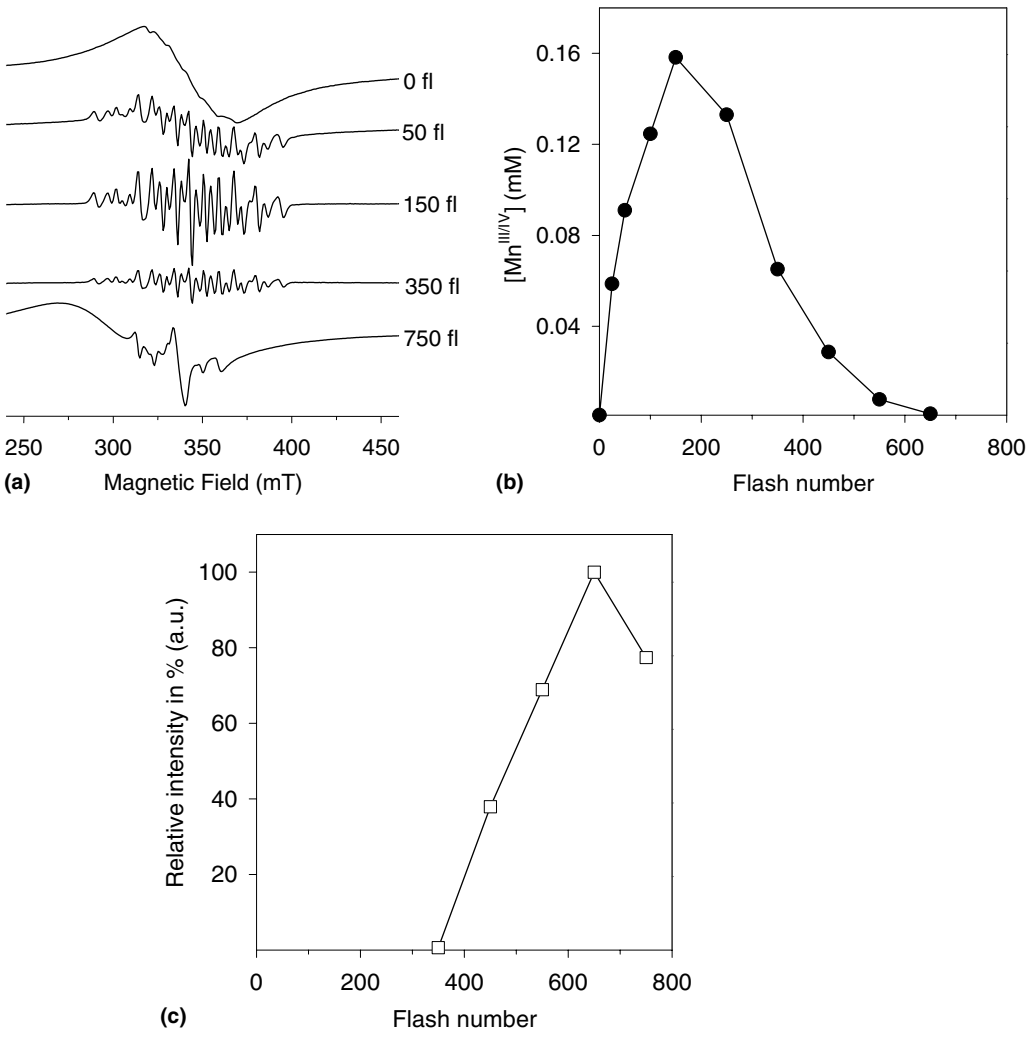

Fig. 5. The result of photo-induced oxidation of **2** with $Ru_2^{II}(bpy)_3$ and Co^{III} in water:acetonitrile = 1:1. (a) Selected EPR spectra after the sample had been exposed to 0, 50, 150, 350 and 750 laser flashes. The appearance and increase of the signal from $Mn_2^{III,IV}$ is observable in the spectra after 50 and 150 flashes. The subsequent decrease of $Mn_2^{III,IV}$ is observed after 350 flashes. The spectrum after 750 flashes shows a radical signal that appeared after extensive flashing. EPR settings are as in Fig. 1(a). (b) Flash number dependent build up and disappearance of the $Mn_2^{III,IV}$ state. (c) Formation of the radical spectrum in the course of the photolysis experiment. The data in (b) and (c) are from the spectra shown in (a) and from other spectra recorded in the same experiment.

flashes, is of Mn origin, the oxidation of $Mn_2^{III,IV}$ would result in formation of the $Mn_2^{IV,IV}$ valence state. $Mn_2^{IV,IV}$, similar to $Mn_2^{III,III}$, is an integral spin system and expected to be EPR silent when the manganese ions are strongly coupled. Thus, it is very likely that further photo-induced oxidation of $Mn_2^{III,IV}$ in **2** resulted in formation of the $Mn_2^{IV,IV}$ valence state.

To ensure that the decrease of the $Mn_2^{III,IV}$ signal is photo-induced and not just a time dependent decay of the $Mn_2^{III,IV}$, an identical sample that had been exposed to 150 flashes was annealed at room temperature for 10 min in the dark. EPR spectra recorded before and after the annealing were compared and revealed that no significant changes in the $Mn_2^{III,IV}$ signal intensity had occurred (not shown). Thereby, we conclude that the decrease of the $Mn_2^{III,IV}$ signal after 150 flashes was indeed light-induced.

3.5. Formation of a radical species

After 450–550 flashes, a new spectral feature appeared that was superimposed on the remaining small fraction of the $Mn_2^{III,IV}$ spectrum. The new spectrum is a radical EPR signal, and is more clearly seen in the spectrum after 750 flashes (Fig. 5(a)). Together with this radical, a very small 6-line EPR signal from Mn appeared in the spectrum (Fig. 5, spectrum 750 fl). The signal is different from the Mn^{II} signal in the dark sample and the origin of this signal is at present unclear.

The new radical EPR signal is magnified in the inset in Fig. 6. The radical signal has $g \sim 2.0046$ and a line width of 8 mT. The g-value is typical for a deprotonated phenol radical [34] and indicates that the radical resides in the ligand of **2**. A microwave power saturation study was performed to determine the relaxation characteris-

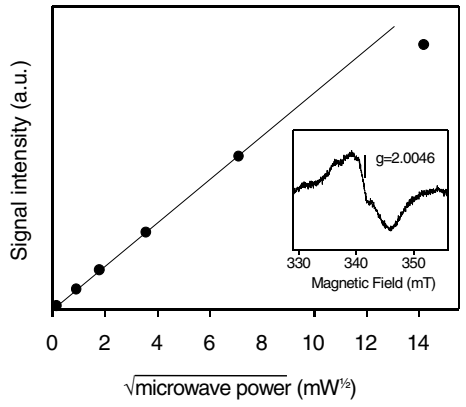

Fig. 6. Microwave power dependence of the amplitude of the radical signal appearing in the photo-oxidation of **2** (compare Fig. 5(a)). The radical signal in the 750 flash sample (Fig. 5(a)) was recorded using different microwave powers at 15 K, using 0.5 mT modulation amplitude. The plot shows the signal intensity versus the square root of the applied microwave power. The points are simply connected by a straight line. Within our available microwave power range (maximum 200 mW) the radical is not saturated to any appreciable extent. The inset shows a magnification of the radical signal recorded at 15 K using 0.02 mW microwave power and 0.5 mT field modulation amplitude. The microwave frequency was 9.52 GHz.

tics of the radical. A plot of the radical intensity versus the square root of microwave power at 15 K is shown in Fig. 6. [2]At all microwave powers up to >100 mW, the signal intensity increases linearly with the square root of the microwave power. Potentially it bends somewhat at higher microwave powers but our maximal available microwave power (200 mW in our instrument) does not allow determination of a precise $P_{1/2}$ value at 15 K. However, it is clear that very high microwave powers are needed to reach microwave saturation for this radical species. This is abnormal for a radical species of organic origin at this temperature. It reflects that the radical has enhanced relaxation, most likely due to magnetic interaction between the radical and manganese. We, thus, suggest that the very fast relaxing radical signal, observable after 500–750 flashes, is formed by ligand oxidation, when one or both of the manganese ions are still bound to the ligand.

4. Discussion

Complex **1** was earlier shown to maintain oxidation states between $Mn_2^{II,II}$ and $Mn_2^{III,III}$ in neat acetonitrile while it was possible to reach also the $Mn_2^{III,IV}$ state during photo-chemical oxidation in the presence of water [21]. However, we could not observe any light-induced intermediates between $Mn_2^{II,II}$ and $Mn_2^{III,IV}$, thus leaving important steps in the reaction unresolved. Complex **2** was found to assume all oxidation states between $Mn_2^{II,III}$ and $Mn_2^{III,IV}$. We also had indications that $Mn_2^{II,II}$ and potentially $Mn_2^{IV,IV}$ could be obtained electrochemically [26]. However, photolysis of **2** in the presence of water was not attempted. The present contribution extends our earlier results as we now identify intermediates in the stepwise oxidation of **1** and also show that **2** can reach several highly oxidized states in sequential photo-induced oxidation reactions [20,21,26].

The samples obtained during photo-induced oxidation of **1** or **2** often contain Mn-dimers in several oxidation states of which, some give rise to EPR spectra. Thereby, we could follow the $Mn_2^{II,II}$, $Mn_2^{II,III}$ and $Mn_2^{III,IV}$, and even further oxidized states. Complex **1** is synthesized in the $Mn_2^{II,II}$ state, which is an integral spin system with a total spin of $S = 5$. Despite this, the weak anti-ferromagnetic coupling of the two Mn^{II} ions ($J = 9.6\ cm^{-1}$) results in population of the spin triplet and quintet states at temperatures around and above 10 K, and transitions from both states contribute to the EPR spectrum [29,30]. In the spin ladders these states lie just above the singlet ground state and care must be taken to select the optimal measuring temperature. We have chosen 12 K to monitor the $Mn_2^{II,II}$ signal. Among the many transitions, well described in [30], the distinct peak at 261 mT was chosen to quantify **1** in the $Mn_2^{II,II}$ state.

$Mn_2^{II,III}$ and $Mn_2^{III,IV}$ are half-integral spin systems, with $S = 1/2$ as the ground state. In the $Mn_2^{II,III}$ state of **1**, the Mn ions are weakly anti-ferromagnetically coupled, with $J = -12.0\ cm^{-1}$ [25]. At 4 K, the ground state is mostly populated and gives good signal intensity, while there is negligible contribution from $Mn_2^{II,II}$ (see above). At 12 K, it is easy to distinguish $Mn_2^{III,IV}$ from $Mn_2^{II,II}$ from their different spectral widths. It is more difficult to distinguish $Mn_2^{II,III}$ and $Mn_2^{III,IV}$. In general, the exchange coupling in dimeric $Mn_2^{III,IV}$ complexes is stronger than for $Mn_2^{II,III}$ complexes. This results in larger separation between the spin ground state and the first excited state. Thus, the spin ground state is still reasonably populated even at 12 K for $Mn_2^{III,IV}$, while the lowest excited state in $Mn_2^{II,III}$ starts to be populated and the ground state is depopulated. To resolve the two valence states, we followed the $Mn_2^{II,III}$ and $Mn_2^{III,IV}$ EPR signals, in spectra recorded at 4 or 12 K. The EPR signal from $Mn_2^{III,IV}$ contributes to the spectra at both 4 and 12 K. However, at 4 K even the weaker lines in the $Mn_2^{II,III}$ spectrum are large enough in the high-field wing of the spectrum (rasterized in Fig. 3) to allow clean analysis.

In our earlier study of **1**, we did not observe $Mn_2^{II,III}$ but indirect evidence indicated that it should be formed

[2] $P_{1/2}$ as defined in formula (1) [35], is commonly used to indicate the relaxation properties of the spin center.

$$I = (I_0\sqrt{P})/\sqrt{(1 + P/P_{1/2})}, \quad (1)$$

where P is the microwave power, $P_{1/2}$ is the half saturation power, I is the measured intensity and I_0 is the calculated unsaturated signal intensity.

with high yield. Therefore, we have now investigated the results of the very first few flashes in the flash train (Figs. 1 and 2). We measured all samples at several temperatures. We also added acetate buffer to affect ligand exchange reactions during the oxidation of **1**. Already the first flash resulted in significant oxidation of **1**. During the first 2–4 flashes, we could correlate the disappearance of $Mn_2^{II,II}$ and formation of $Mn_2^{II,III}$. After 4 flashes, $Mn_2^{II,III}$ had reached its peak concentration and then it started to decline. The observation of $Mn_2^{II,III}$ is most likely affected by the presence of an excess of acetate (200 mM) in the experiment and we attribute this effect to bridging ligand modification, which will be discussed below.

Presumably, $Mn_2^{II,III}$ was then oxidized one step to $Mn_2^{III,III}$ but finding direct evidence for this is difficult. However, an appreciable fraction of **1** is not observed in the EPR spectra and a quantitative calculation after 8 flashes (from Fig. 2) shows that almost 55% of **1** was present in an EPR silent state. It is highly likely that much of this is $Mn_2^{III,III}$ at least after the 2–8 initial flashes.

The detection of $Mn_2^{III,IV}$ provides direct evidence for the three step oxidation of **1**. It is not impossible that an even higher oxidation state (i.e., $Mn_2^{IV,IV}$) can be formed during continued flashing of the sample. However, this state is transient and ends with the formation of MnO_2 (Mn^{IV}), which implies that the $Mn_2^{IV,IV}$ state is unstable in **1**.

Photo-induced oxidation of **1** in pure acetonitrile resulted in a high yield of the $Mn_2^{II,III}$ state, which indicates an efficient conversion from $Mn_2^{II,II}$ to $Mn_2^{II,III}$ also in the absence of water. We can, thus, conclude with confidence that the $Mn_2^{II,III}$ state is an intermediate in the course of multistep photo-oxidation of **1**. It also reinforces that the redox potentials of the $Mn_2^{II,II}/Mn_2^{II,III}$ couple are well separated from the $Mn_2^{II,III}/Mn_2^{III,III}$ couple, which is in agreement with the determined redox potentials ($E_{1/2} = 0.5$ and 1.06 V vs. SCE, respectively, see [26]). In contrast to water containing solution, it was not possible to reach $Mn_2^{III,IV}$ by light in neat acetonitrile, reflecting that this oxidation occurs at a higher potential than available from Ru^{III} [21].

Comparing the present study and our previous work, it appears that the detection of $Mn_2^{II,III}$ in **1** by EPR very much depends on the solvent and on the presence of acetate. From the limited data in our earlier study, we suggested a ligand exchange model in which the acetate-in **1** were replaced by μ-oxo- or μ-hydroxo-bridges in higher oxidation states. This was tentatively proposed to occur in the $Mn_2^{III,III}$ state. A recent EXAFS study shows that the intermanganese distance of ~3.4 Å in the initial $Mn_2^{II,II}$ state was essentially unchanged upon electrochemical generation of $Mn_2^{II,III}$ in neat acetonitrile, but was considerably shortened to ~2.9 Å upon the second oxidation to the $Mn_2^{III,III}$ state [A. Magnuson, H. Dau, et al., in preparation]. An explanation for the difference in Mn–Mn distances requires a change in bridging mode in $Mn_2^{III,III}$. However, although the bridging mode is completely transformed in $Mn_2^{III,III}$, it may depend on changes taking place already in $Mn_2^{II,III}$.

We can now propose a clearer picture of why $Mn_2^{II,III}$ escaped detection in our earlier work. Two combined effects can explain this. First we may simply have overlooked $Mn_2^{II,III}$ earlier, since it was formed in much lower concentration (maximum ca. 50 μM, Fig. 6 in [21]) than in our present study (ca. 0.15 mM, Fig. 2). The reason for the observed high concentration in the present study is found in the ligand exchange reactions. Our earlier results indicate that a change in bridging mode is a prerequisite for stabilization of $Mn_2^{III,III}$. Acetato bridges in dinuclear metal complexes are in general easily exchanged to other ligand molecules and this has earlier been shown to also occur in Mn-compounds [22,36,37]. One possibility is that the rapid association/dissociation equilibrium of the acetato bridges in the presence of water facilitates the oxidation from $Mn_2^{II,III}$ to $Mn_2^{III,III}$ by assisting the bridge modifications. Therefore, $Mn_2^{II,III}$ may escape detection due to low steady state concentrations. This was the situation in our earlier study, while in our present work the addition of acetate "locks" some of **1** into a $Mn_2^{II,III}$ form which is less readily oxidized, and consequently the total concentration of $Mn_2^{II,III}$ at any one instant is much higher.

There is another plausible explanation for our inability to observe the $Mn_2^{II,III}$ in the absence of acetate. This involves the structural differences in the $Mn_2^{II,III}$ state of **1** with or without μ-acetato bridges, which most likely induces differences in exchange interaction. Even small changes in bridging mode between complex bound metal ions are known to change the magnetic coupling, leading to line broadening in the EPR spectrum to the extent that it becomes hard to detect. In either case, the circumstances for the formation of the $Mn_2^{II,III}$ state in **1**, i.e., solvent and acetate concentration, are critical for observing the $Mn_2^{II,III}$ EPR signal. In this respect it is important that the EPR spectra of $Mn_2^{II,III}$ in water/acetonitrile in presence of acetate and in neat acetonitrile are identical (Fig. 3). This provides strong evidence that this EPR signal indeed originates from complexes that do have the acetate ligands, i.e., prior to the proposed ligand exchange reactions with water have occurred (this argument was pointed out to us by one of the referees and we gratefully acknowledge this).

Complex **2** has been synthesized with the idea that the phenolate ligands shall stabilize higher oxidation states than the pyridyl ligand in **1**. This is vital in attempts to manage water oxidation or to mimic the natural WOC in PSII, which has a large set of oxygen ligands provided mainly from carboxylic amino acid side chains on the donor side of PSII [6].

Here, we describe completely new results from flash-photolysis experiments of **2** in the presence of water. Also in this case we observed stepwise photo-induced oxidation. The flash-dependent appearance and subsequent increase of the $Mn_2^{III,IV}$ EPR signal is indicative of the first oxidation step from $Mn_2^{III,III}$ to $Mn_2^{III,IV}$. After that, the EPR signal gradually declined without any sign of side reactions. In analogy to the situation in **1**, where the EPR invisible $Mn_2^{III,III}$ state was formed, we interpret this as a second oxidation of **2** resulting in the $Mn_2^{IV,IV}$ state which is also EPR invisible. In contrast to the situation in **1**, the $Mn_2^{IV,IV}$ state in **2** seems relatively stable under our experimental conditions. Neither MnO_2 nor any free Mn^{II} formed during appreciable times (5–10 min at room temperature) from the presumed $Mn_2^{IV,IV}$ state. In addition, further photo-induced oxidation led to the formation of a fast-relaxing radical (discussed below).

At a first glance, the yield of photo-induced oxidation of **2**, viewed as the number of laser flashes needed to accomplish one-step oxidation, seems lower than in **1**. However, to a large degree this reflects the lower concentration of Co^{III}, the electron acceptor used in the experiments with **2** which inevitably reduces the yield of photo-oxidation of $Ru^{II}(bpy)_3$. To some degree, the lower yield also reflects the higher redox potential of the first oxidation of **2** as compared to **1** [21,26]. In our present work, our focus was directed on driving **2** to high valence states via photo-oxidation, which is an important issue for mimicking the WOC in PSII. However, an important property of **2** is that it also can be electrochemically reduced from the synthesized $Mn_2^{III,III}$ state to $Mn_2^{II,III}$ and further to $Mn_2^{II,II}$ [26]. Accordingly, **2** can accommodate at least five Mn-centered oxidation states from $Mn_2^{II,II}$ to $Mn_2^{IV,IV}$, and potentially one more oxidation involving radical formation in the ligand.

The EPR spectra of **1** and **2** in the $Mn_2^{III,IV}$ state reveals different features in terms of spectral width and hyperfine pattern. The EPR spectrum from $Mn_2^{III,IV}$ in **2** is 106 mT wide, which is significantly narrower than that of 122 mT from **1**. The hyperfine structure in the spectrum of **2** shows a well-resolved 23-line pattern, while a typical 16-line hyperfine pattern is seen in **1**. The hyperfine pattern in **1** arises due to strong anti-ferromagnetic coupling in $Mn_2^{III,IV}$ which leads to an effective spin of $S = 1/2$. The "typical" 16-line pattern is observed in most $Mn_2^{III,IV}$ complexes, where the spin projection of the Mn^{III} ion is about twice that of Mn^{IV}, as an effect of the considerable zero-field splitting (ZFS) of Mn^{III} [38]. This typical relationship may not hold for complex **2**, where the phenolic ligand most likely introduces a distortion, which can alter the ZFS of the Mn^{III} ion. Another factor, which might have an influence on the hyperfine pattern, is the exchange coupling between the Mn ions. However, according to EXAFS data obtained from **2** in the $Mn_2^{III,IV}$ state [A. Magnuson, H. Dau, et al., in preparation], the complex has obtained at least one μ-oxo bridge upon oxidation, which ensures a strong anti-ferromagnetic coupling. The exact nature of the spin projection in Mn^{III} relative to Mn^{IV}, or any detailed description of the altered hyperfine coupling, is beyond the scope of the present work.

The radical formed in **2** is interesting. It is formed late during the photo-oxidation and from the results it seems that it was not formed directly from the $Mn_2^{III,IV}$ state. Instead, $Mn_2^{III,IV}$ had disappeared almost completely before the radical had reached appreciable amplitudes (Fig. 5). This is best seen from the relative amplitudes in the samples where 350 or 450 flashes were given. The signal from $Mn_2^{III,IV}$ then decreased to 40% and 17% of its maximum amplitude, respectively, while the radical signal was absent in the 350 flash sample, and reached ca. 35% of its maximum in the 450 flash sample (Fig. 5(b) and (c)). Therefore, we conclude that the radical is formed by continued flash-induced oxidation of **2** after it reached $Mn_2^{IV,IV}$.

What is then the nature of this radical? The obtained g value of 2.0046 resembles well the typical g value of a neutral phenol radical [34]. Thus, the radical probably originates from one of three phenolates in the ligand that normally are coordinated to the Mn ions in **2** (Scheme 1). Release of manganese is a frequent result of excessive oxidation, e.g., by bulk electrolysis, of complexes like **1** and **2** [21,26]. Since EPR is very sensitive to Mn^{II}, the very small amplitude of this signal in the EPR spectra of **2** containing the radical (Fig. 5, 750 fl) suggests that most manganese remained coordinated to the ligand. Consequently, the formation of a radical species implies that the oxidation of the manganese moiety in **2** probably reached its limit, $Mn_2^{IV,IV}$, and that the ligand is then accessible for oxidation by the potential generated by Ru^{III}(+1.26 V vs. NHE).

There are two remarkable characteristics of this radical, the broad line width (8 mT) and the very fast relaxation ($P_{1/2}$ higher than we can measure at 15 K). Ordinarily phenol or tyrosine radicals are much narrower (~1 mT) and relax much slower ($P_{1/2}$ at 15 K on the μW scale). However, phenol radicals in conjunction with metal ions have been reported to give rise to broad EPR signals [46]. The fast relaxation probably also reflects that the radical is in the vicinity of manganese still associated to the ligand. Examples from nature are found in PSII, which contains two redox active tyrosines. Tyr_Z is situated 7–10 Å away from the manganese cluster in the WOC. It relaxes extremely fast [39,40] and sometimes gives rise to fast relaxing, split or broadened EPR signals due to interactions between the radical and the manganese cluster [41–44]. The exact shape of the interaction signal depends on the spin state of the manganese cluster [42,44,45]. It is noteworthy that similar split interaction signals between a dinuclear

$Mn_2^{III,IV}$ complex and a nitronyl nitroxide (NIT) radical have been observed in synthetic compounds also [46]. Also the other redox active tyrosine in PSII, Tyr_D interacts magnetically with the manganese cluster [47–49]. This tyrosine is situated ca. 30 Å from the manganese cluster and is involved in slow redox reactions in PSII. When the manganese cluster is present, the relaxation of the Tyr_D radical is much enhanced (despite the rather long distance). The relaxation enhancement depends heavily on the S-state, reflecting the magnetic coupling to the manganese cluster. If the manganese cluster is removed, the relaxation of Tyr_D is slower and resembles free organic radicals. In contrast to Tyr_Z, Tyr_D has never been reported to become broadened or split through its magnetic interactions with the manganese cluster, due to the long Tyr–Mn distance.

Through the above analogies with the tyrosine radicals in PSII, we can conclude that our phenolic radical in **2** is broadened and fast relaxing due to magnetic interaction with one or more manganese ions still coordinated to the ligand. Albeit being very close, the magnetic interactions between the paramagnetic centers are not strong enough to give rise to a split signal of the type observed for Tyr_Z in PSII or in the NIT-containing Mn complex [46]. Instead, the relatively weak coupling may reflect the spin state of the manganese, which we have proposed is in the $Mn_2^{IV,IV}$ valence state. An integer spin system such as this where the two Mn^{IV} ions are strongly anti-ferromagnetically coupled, leading to an EPR silent spin state, would most likely not broaden the radical as much as an $S = 1/2$ system due to the lack of a strong exchange interaction.

Keeping in mind that the tyrosyl radical ($Y_Z^{\cdot}$) in PSII plays a vital role for the catalysis of water oxidation, it is interesting to note that **2** has the capacity to store several oxidizing equivalents and form a neutral phenol radical close to the metal site, in a fashion strikingly similar to the WOC.

5. Conclusions

The multistep photo-induced oxidations of **1** and **2** resulting in oxidation states $Mn_2^{III,IV}$ and $Mn_2^{IV,IV}$ in **1** and **2**, respectively, mimic major aspects of the catalytic cycle of the WOC in PSII. Formation of the $Mn_2^{IV,IV}$ state, and one further oxidation step involving ligand oxidation, is suggested in **2**. We have also successfully observed $Mn_2^{II,III}$ in **1**, in the presence of excessive amounts of acetate. This suggests a modification of the bridging mode, where one or both of the bridging acetates in **1** is in equilibrium with formation of a μ-oxo or a μ-hydroxo bridge. The equilibrium favors the modified bridge in the presence of high amounts of water, and in reverse the acetate-bridge is favored in the presence of high concentration of acetate. We suggest that the change in bridging mode facilitates the oxidation of the $Mn_2^{II,III}$ to the EPR silent $Mn_2^{III,III}$ state. A similar ligand modification model is also proposed for **2**, where the $Mn_2^{III,IV}$ state is suggested to contain one or two μ-oxo-bridges. The fact that the Mn coordination sphere of **2** stabilizes the higher oxidation state is demonstrated by photo-induced oxidation of **2**, where $Mn_2^{IV,IV}$ can be obtained.

6. Abbreviations

bpmp	2,6-bis[[*N*,*N*-di(2-pyridylmethyl)amino]methyl]-4-methylphenol
bpy	bipyridine
Co^{III}	*Penta*-amminechlorocobalt(III) chloride
EPR	electron paramagnetic resonance
EXAFS	extended X-ray absorption fine structure
NHE	natural hydrogen electrode
NIT	nitroxide nitroxyl
P_{680}	the primary electron donor in PSII
PSII	photosystem II
$Ru^{II}(bpy)_3$	ruthenium-*tris*-bipyridine
SCE	saturated calomel electrode
Tyr_D	tyrosine-D (Tyr161 on the D2 protein in PSII)
Tyr_Z	tyrosine-Z (Tyr161 on the D1 protein in PSII)
WOC	water oxidizing complex
ZFS	zero-field splitting
4-NBB	4-Nitrobenzyl bromide

Acknowledgements

Financial support from the Swedish National Energy Administration, the Swedish Research Council, The Knut and Alice Wallenberg Foundation and DESS are gratefully acknowledged. M.F.A. was supported from the Swedish Foundation for Strategic Research. The authors also gratefully acknowledge valuable discussions with Dr. R. Lomoth and Dr. L. Hammarström, Uppsala University, and Prof. B. Åkermark, Stockholm University.

References

[1] L. Sun, L. Hammarström, B. Åkermark, S. Styring, Chem. Soc. Rev. 30 (2001) 36–49.
[2] J. Barber, Curr. Opin. Struct. Biol. 12 (2002) 523–530.
[3] B.A. Diner, F. Rappaport, Annu. Rev. Plant. Biol. 53 (2002) 551–580.
[4] R.D. Britt, in: D.R. Ort, C.F. Yocum (Eds.), Oxygenic Photosynthesis: The Light Reactions, Kluwer Academic Publishers, Dordrecht, 1996, pp. 137–164.
[5] B.A. Diner, G.T. Babcock, in: D.R. Ort, C.F. Yocum (Eds.), Oxygenic Photosynthesis: The Light Reactions, Kluwer Academic Publishers, Dordrecht, 1996, pp. 213–247.

[6] R.J. Debus, in: A. Sigel, H. Sigel (Eds.), Metal Ions in Biological Systems, Marcel Dekker, New York, 2000, pp. 657–710.
[7] V.K. Yachandra, K. Sauer, M.P. Klein, Chem. Rev. 96 (1996) 2927–2950.
[8] C. Tommos, G.T. Babcock, Biochim. Biophys. Acta 1458 (2000) 199–219.
[9] J.H. Robblee, R.M. Cinco, V.K. Yachandra, Biochim. Biophys. Acta 1503 (2001) 7–23.
[10] H. Dau, Lu. Iuzzolino, J. Dittmer, Biochim. Biophys. Acta 1503 (2001) 24–39.
[11] J. Messinger, Biochim. Biophys. Acta 1459 (2000) 481–488.
[12] K.A. Åhrling, S. Styring, in: M. Yunus, P. Mohanty, U. Pathre (Eds.), Probing Photosynthesis, Taylor & Francis, London, 2000, pp. 148–163.
[13] D. Kuzek, R.J. Pace, Biochim. Biophys. Acta 1503 (2001) 123–137.
[14] W. Hillier, T. Wydrzynski, Biochemistry 39 (2000) 4399–4405.
[15] K.L. Clemens, D.A. Force, R.D. Britt, J. Am. Chem. Soc. 124 (2002) 10921–10933.
[16] V.V. Klimov, S.V. Baranov, Biochim. Biophys. Acta 1503 (2001) 187–196.
[17] L. Sun, H. Berglund, R. Davydov, T. Norrby, L. Hammarström, P. Korall, A. Börje, C. Philouze, K. Berg, A. Tran, M. Andersson, G. Stenhagen, J. Mårtensson, M. Almgren, S. Styring, B. Åkermark, J. Am. Chem. Soc. 119 (1997) 6996–7004.
[18] D. Burdinski, K. Wieghardt, S. Steenken, J. Am. Chem. Soc. 121 (1999) 10781–10787.
[19] D. Burdinski, E. Bothe, K. Wieghardt, Inorg. Chem. 39 (2000) 105–116.
[20] L. Sun, M.K. Raymond, A. Magnuson, D. LeGourriérec, M. Tamm, M. Abrahamsson, P.H. Kenéz, J. Mårtensson, G. Stenhagen, L. Hammarström, S. Styring, B. Åkermark, J. Inorg. Biochem. 78 (2000) 15–22.
[21] P. Huang, A. Magnuson, R. Lomoth, M. Abrahamsson, M. Tamm, L. Sun, B. van Rotterdam, J. Park, L. Hammarström, B. Åkermark, S. Styring, J. Inorg. Biochem. 91 (2002) 159–172.
[22] A.E.M. Boelrijk, S.V. Khangulov, C.G. Dismukes, Inorg. Chem. 39 (2000) 3009–3019.
[23] H. Diril, H.-R. Chang, X. Zhang, S.K. Larsen, J.A. Potenza, C.G. Piepont, H.J. Schugar, S.S. Isied, D.N. Hendrickson, J. Am. Chem. Soc. 109 (1987) 6207–6208.
[24] H.-R. Chang, S.K. Larsen, P.D.W. Boyd, C.G. Pierpont, D.N. Hendrickson, J. Am. Chem. Soc. 110 (1988) 4565–4576.
[25] H. Diril, H.R. Chang, M.J. Nilges, X.H. Zhang, J.A. Potenza, H.J. Schugar, S.S. Isied, D.N. Hendrickson, J. Am. Chem. Soc. 111 (1989) 5102–5114.
[26] R. Lomoth, P. Huang, J. Zheng, L. Sun, L. Hammarström, B. Åkermark, S. Styring, Eur. J. Inorg. Chem. (2002) 2965–2974.
[27] B.P. Sullivan, D.J. Salmon, T.J. Meyer, Inorg. Chem. 17 (1978) 3334–3341.
[28] R. Manchanda, G.W. Brudvig, R.H. Crabtree, N. J. Chem. 18 (1994) 561–568.
[29] S.V. Khangulov, P.J. Pessiki, V.V. Barynin, D.E. Ash, G.C. Dismukes, Biochemistry 34 (1995) 2015–2025.
[30] S. Blanchard, G. Blondin, E. Rivière, M. Nierlich, J.-J. Girerd, Inorg. Chem. 42 (2003) 4568–4578.
[31] S.V. Khangulov, V.V. Barynin, N.V. Voevodskaya, A.I. Grebenko, Biochim. Biophys. Acta 1020 (1990) 305–310.
[32] P.J. Pessiki, S.V. Khangulov, G.C. Dismukes, J. Am. Chem. Soc. 116 (1994) 891–897.
[33] K.-O. Schäfer, R. Bittl, W. Zweygart, F. Lendzian, G. Haselhorst, T. Weyhermüller, K. Wieghardt, W. Lubitz, J. Am. Chem. Soc. 120 (1998) 13104–13120.
[34] A. Magnuson, H. Berglund, P. Korall, L. Hammarström, B. Åkermark, S. Styring, L. Sun, J. Am. Chem. Soc. 119 (1997) 10720–10725.
[35] H. Rupp, K.K. Rao, D.O. Hall, R. Cammack, Biochim. Biophys. Acta 537 (1978) 255–269.
[36] T. Tanase, S.J. lippard, Inorg. Chem. 34 (1995) 4682–4690.
[37] K. Wieghardt, U. Bossek, B. Nuber, J. Weiss, J. Bonvoisin, M. Corbella, S.E. Vitols, J.J. Girerd, J. Am. Chem. Soc. 110 (1988) 7398–7411.
[38] M. Zheng, G.C. Dismukes, Inorg. Chem. 35 (1996) 3307–3319.
[39] B.J. Hallahan, J.H.A. Nugent, J.T. Warden, M.C.W. Evans, Biochemistry 31 (1992) 4562–4573.
[40] L.-E. Andréasson, I. Vass, S. Styring, Biochim. Biophys. Acta 1230 (1995) 155–164.
[41] A. Boussac, J.L. Zimmermann, A.W. Rutherford, Biochemistry 28 (1989) 8984–8989.
[42] K.V. Lakshmi, S.S. Eaton, G.R. Eaton, H.A. Frank, G.W. Brudvig, J. Phys. Chem. B 102 (1998) 8327–8335.
[43] P. Dorlet, M.D. Valentin, G.T. Babcock, J.L. McCracken, J. Phys. Chem. B 102 (1998) 8239–8247.
[44] J.H.A. Nugent, I.P. Muhiuddin, M.C.W. Evans, Biochemistry 41 (2002) 4117–4126.
[45] C. Zhang, S. Styring, Biochemistry 42 (2003) 8066–8076.
[46] D.S. Marlin, E. Bill, T. Weyhermüller, E. Rentschler, K. Wieghardt, Angew. Chem., Int. Ed. 41 (2002) 4775–4779.
[47] S. Styring, A.W. Rutherford, J. Am. Chem. Soc. 27 (1988) 4915–4923.
[48] R.G. Evelo, S. Styring, A.W. Rutherford, A.J. Hoff, Biochim. Biophys. Acta 973 (1988) 428–442.
[49] D. Koulougliotis, D.J. Hirsh, G.W. Brudvig, J. Am. Chem. Soc. 114 (1992) 8322–8323.